

CFTR-dependent Cl^- secretion in *Xenopus laevis* lung epithelium

Dagmar Sommer^a, Roman Bogdan^a, Jens Berger^a, Dorothea M. Peters^b,
Rory E. Morty^b, Wolfgang G. Clauss^a, Martin Fronius^{a,*}

^a Institute of Animal Physiology, Justus-Liebig University of Giessen, Wartweg 95, 35392 Giessen, Germany

^b Department of Internal Medicine II, Justus-Liebig University of Giessen, Aulweg 123, D-35392 Giessen, Germany

Accepted 26 March 2007

Abstract

In our present study we used preparations from *Xenopus laevis* lungs to perform electrophysiological Ussing chamber measurements, uni-directional flux measurements, and employed molecular approaches to elucidate the presence and function of a cystic fibrosis transmembrane conductance regulator (CFTR) homolog in this tissue. Application of different CFTR blockers (NPPB (5-nitro-2-(3-phenylpropylamino)benzoic acid), niflumic acid (NFA), glibenclamide, lonidamine, CFTR_{inh}-172) to the apical side of the tissues was able to significantly decrease the measured short circuit current (I_{SC}) indicating a Cl^- secretion due to luminal located CFTR channels. This was further supported by a net $^{36}\text{Cl}^-$ secretion determined by radioactive tracer flux experiments. Further, *Xenopus* pulmonary epithelia responded to apical chlorzoxazone exposure – a CFTR activator – and this activated current was inhibited by CFTR_{inh}-172. We performed reverse transcription-PCR (RT-PCR) and Western blot analysis and with both approaches we found characteristic signals indicating the presence of a CFTR homolog in *Xenopus* lung. In addition, we were able to detect CFTR in apical membranes of *Xenopus* lung slices with immunohistological techniques. We conclude that *Xenopus* lung epithelium exhibits functional CFTR channels and that this tissue represents a valuable model for the investigation of ion transport properties in pulmonary epithelia. © 2007 Elsevier B.V. All rights reserved.

Keywords: Alveolar ion transport; Alveolar epithelium; Pulmonary ion transport; Transepithelial ion transport; Ussing chamber; Frog lung; *Xenopus laevis*; Chloride channel; Chloride channel blocker; CFTR; Reverse transcription-PCR; Immunofluorescence; Radioactive flux measurements; $^{36}\text{Cl}^-$

1. Introduction

The lung surface of air breathing vertebrates is lined by an epithelium that forms a barrier separating the external environment from the internal milieu. This barrier function is facilitated by a liquid surface layer, which covers the entire luminal surface of the respiratory tract (Boucher, 2003).

This liquid layer consists of a mucous layer and a layer of periciliary fluid, separated by surfactant proteins (Rubin, 2002) and represents the first barrier against inhaled irritants and pathogens to protect the entire organism (Knowles and Boucher, 2002). Further, surfactants decrease the surface tension in the pulmonary alveoli to facilitate gas exchange (Whitsett, 2005). These two functions – effective host defense and sufficient gas exchange – crucially depend on the viscosity as well as on the height of the liquid surface layer. The composition of this

fluid layer is controlled by active transepithelial ion transport conducted by the pulmonary epithelia (Matthay et al., 2002).

It is well accepted that the control of lung fluid content is accomplished by the interaction of Na^+ absorption involving epithelial Na^+ channels (ENaCs, Matalon and O’Broovich, 1999) and Cl^- transport via luminal Cl^- channels, in particular the cystic fibrosis transmembrane conductance regulator (CFTR, O’Grady and Lee, 2003). The net transport of these ions create a transepithelial osmotic gradient, which is the effective driving force for the movement of water across the epithelium and thereby controls the content of fluid in the lung as well as the viscosity of this fluid layer (Matthay et al., 1996).

Malfunctions of pulmonary ion transport are associated with severe diseases in humans. For example, the hyperabsorption of Na^+ and deficient Cl^- secretion observed in patients with cystic fibrosis increases the viscosity of the airway surface layer and thereby hampers mucociliary clearance (Donaldson and Boucher, 2003). This leads to insufficient host defense associated with increased infections and damage to the respiratory tract (Pilewski and Frizzell, 1999). Conversely, formation of

* Corresponding author. Tel.: +49 641 99 35255; fax: +49 641 99 35059.
E-mail address: martin.fronius@bio.uni-giessen.de (M. Fronius).

pulmonary edema – independent of its origin – is associated with decreased water clearance from the airspace due to insufficient ion absorption (Matthay et al., 2005). This leads to fluid accumulation and impaired gas exchange.

Although the participation of CFTR-dependent Cl^- transport in the mammalian pulmonary epithelium is beyond dispute, little is known about its distinct role. In the upper airways and submucosal glands in particular, there is sufficient evidence concerning the participation of CFTR in Cl^- secretion (Devor et al., 2000). In distal airway epithelium as well as in the alveolar epithelia little is known about the function of the CFTR and its contribution to transcellular ion transport. Preliminary studies indicate that CFTR is involved in Cl^- absorption (Fang et al., 2002, 2006), but there is also evidence concerning CFTR mediated Cl^- secretion (Brochiero et al., 2004). One reason for this controversy may be the difficulties in performing transepithelial ion transport studies using isolated cells from the distal lung (e.g. alveolar cells), since in some cases cells of uncertain phenotypes have been used (Lazrak et al., 2000a). Further, several studies have demonstrated that the ion transport properties of isolated alveolar cells may vary depending on the culture conditions (Dobbs, 1990; Kunzelmann et al., 1996; Jain et al., 2001).

In the present study, freshly isolated *Xenopus laevis* lungs were employed for ion transport studies. An important feature of this organ is its simple, sac-like structure. This relatively simple anatomy makes this organ suitable for transepithelial Ussing chamber recordings permitting measurements on a native epithelium with intact cell–cell interactions. Prior studies have clearly demonstrated similarities concerning the morphology of the air–blood barrier between amphibian and mammalian alveolar epithelia (Meban, 1973; Dierichs, 1975; Fischer et al., 1989). Further, there are substantial similarities between the *Xenopus* lung and mammalian pulmonary epithelia concerning the basic transepithelial ion transport properties involving apical ENaCs (Fischer et al., 1989; Kim, 1990; Baxendale-Cox, 1999), basolateral Na/K-ATPase (Fischer and Clauss, 1990; Illek et al., 1990) and basolateral K^+ channels (Ilek et al., 1990)—the main components of sodium absorbing epithelia following the two-membrane hypothesis developed by Koefoed-Johnson and Ussing (1958).

Here, we present evidence concerning a luminal Cl^- secretion in this tissue, which was sensitive to common CFTR inhibitors (NPPB, NFA, glibenclamide, lonidamine and CFTR_{inh}-172; Schultz et al., 1999; Ma et al., 2002) and could be augmented by the CFTR activator chlorzoxazone (Singh et al., 2000; Cuthbert, 2001). The presence of a putative CFTR ion channel in this tissue is further supported by reverse transcription-PCR, Western blot analysis and immunofluorescence.

2. Materials and methods

2.1. Animals and tissue preparation

Lungs of adult female South African clawed frogs (*X. laevis*) were used for this study. The animals were purchased from H. Kaehler (Hamburg, Germany), kept in tap water and fed once

a week with commercial fish-food. Most of the used animals were injected 48 and 24 h before killing with adrenocorticotrophic hormone (ACTH) to increase basal ion transport rates (Fronius et al., 2004). Further we have performed some experiments with non-ACTH injected animals to ensure that CFTR is not only induced by ACTH injection (immunofluorescence staining, electrophysiological recordings and tracer flux measurements). Preceding removal of the lungs, all animals were hypothermally anaesthetized and killed by decapitation. For Ussing chamber experiments the lungs were incised along the large pulmonary artery and dissected to flat sheets. In order to mount the tissues into Ussing chambers, they were fixed either by a Lucite ring, which was glued from the pleural side, or by a Lucite ring containing pins. Preparations were then mounted in adapted Ussing chambers and bathed from both sides with identical Ringer's solution.

2.2. Electrophysiological recordings

We used adapted 200 μl pipette tips containing 1 M Agar–KCl as holder for the Ag/AgCl wires (surrounded by 1 M KCl) to connect the bath solution with the voltage-clamp amplifier. Solely electrodes with a spontaneous potential difference <1 mV were used for electrophysiological recordings. In a representative series of experiments ($n=6$) ouabain was applied to determine zero current levels. Under these conditions we obtained a putative electrode drift of about 8% with respect to the current values before ouabain application. Since this drift is relative low, the measured values were not corrected. After 3–5 min of equilibration the spontaneous generated transepithelial potential difference (V_T , lumen negative) was clamped to 0 V and the short circuit current (I_{SC}) was recorded continuously. Additional experiments were performed in the open circuit mode, monitoring the transepithelial potential (V_T). In all experiments, tissues were allowed to equilibrate (30–180 min), prior to drug administration. Data were digitized by a MacLab interface (ADInstruments, Australia) and stored on computer (Apple LC II, USA). Additionally, the I_{SC}/V_T was monitored on a strip-chart recorder (Kipp and Zonen, Netherlands). In order to estimate the transepithelial resistance (RT), current/voltage deflections due to voltage/current pulses of 2.5 mV/5 μA (duration 1 s) were determined and used to calculate RT according to Ohm's law. Effective aperture of the chambers used was 0.5 cm^2 . All experiments were performed at room temperature.

2.3. Unidirectional flux measurements

For these recordings tissues were mounted on modified Ussing chambers with an effective aperture of 1 cm^2 and bathed with a volume of 3.5 ml Ringer's solution (composition see below) on each side. Measurements were performed in the open circuit mode as well as in the short circuit mode. Chambers were connected via agar bridges to a voltage-clamp amplifier (Müßler Datentechnik, Germany). After an equilibration period of 90 min $^{36}\text{Cl}^-$ (29 kBq) was added either to the apical or the basolateral side of the tissues. After every 30 min, samples were taken from each side of the chambers to determine effective tracer fluxes

in order to calculate net $^{36}\text{Cl}^-$ fluxes. Solutions were bubbled with compressed air and experiments were performed at room temperature.

2.4. Solutions and chemicals

Generally, symmetrical Ringer's solution (NRS) was applied to both compartments containing: 100 mM NaCl, 3 mM KCl, 1 mM CaCl_2 , mM MgCl_2 , 10 mM glucose and 5 mM HEPES (pH 7.4, adjusted with trizma base). The apical solution was additionally gassed with compressed air containing 20% oxygen, to ensure sufficient oxygen supply to the tissue. The following substances were used in this study: amiloride to inhibit epithelial Na^+ channels; NPPB (5-nitro-2-(3-phenylpropylamino)-benzoate), NFA (niflumic acid), glibenclamide, lonidamine and CFTR_{inh}-172 as designated CFTR inhibitors. All compounds were purchased from Sigma (except NPPB; Tocris) and added from stock to the experimental solution. Except amiloride (water), all blockers were dissolved in DMSO. In order to avoid side effects by the solvent with concentrations >0.2%, equal amounts of DMSO were added to the perfusion solution prior to the blocker application.

2.5. Statistical analyses

Values are given as means \pm standard error of the mean (S.E.M.), n indicates the number of performed experiments. Paired Student's t -test was used to estimate the significance between means (comparing the influence of a compound with values before the compound was added). Significant different means are indicated by * or # and a P -value of at least <0.05 was considered as statistically significant. To determine half-maximal inhibition concentrations (IC_{50}) mean values of at least three applications for each blocker concentration were plotted and fitted by Hill equation.

2.6. Reverse transcription-PCR

Freshly isolated *Xenopus* lungs were frozen and homogenized in liquid nitrogen. Total RNA was extracted with RNeasy[®] Midi Kit (Qiagen) according to the manufacturer's protocol including a DNase digestion step. RNA was reverse transcribed with Oligo-dT primers and the ImProm-II Reverse Transcription Kit (Promega). Negative controls were performed under the same conditions but in the absence of reverse transcriptase. The following PCR was carried out with the GoTaq system (Promega) in a 50 μl sample containing 2 mM MgCl_2 . Specific primers were designed from the published sequence of *Xenopus* CFTR (GenBank accession number X65256). In order to detect contamination with genomic DNA, intron spanning primers were selected. Forward primer sequence was 5'-ATCAGTTTCCAGGACAATTG-3' and reverse primer sequence was 5'-ACCAGAAAGCGCTGGCATTG-3', which amplified a product with an expected size of 259 bp. The protocol for the thermal cycler was as follows: 45 s at 95 °C, 30 s at 55 °C and 45 s at 72 °C for 35 cycles. The product was visualized

on a 2.5% agarose gel and bands of expected size were excised. The amplicon was isolated using the Wizard SV Gel and PCR Clean-Up System (Promega) and ligated into pGEM-TEasy vector (Promega). Plasmid isolation was done with Wizard Plus SV Miniprep kit (Promega). Sequencing confirmed 100% identity to the published sequence of *Xenopus* CFTR.

2.7. Western blots

Frozen *Xenopus* lungs and oocytes, were homogenized in liquid nitrogen, resuspended in lysis buffer (150 mM NaCl, 20 mM Tris, 1 mM EDTA, 1 mM EGTA and 0.5% IGEPAL[®] CA-630, Na_3VO_4 (10 $\mu\text{l}/\text{ml}$ lysis buffer), Complete[™] (40 $\mu\text{l}/\text{ml}$ lysis buffer)) for approximately 10–15 min and dispersed via a syringe. Following centrifugation for 15 min at 4 °C (13,000 rpm) 20 μl of each sample was separated on 10% SDS-polyacrylamide gels and transferred to polyvinylidene difluoride (PVDF) membranes. To avoid unspecific binding, membranes were incubated for 1 h with 5% non-fat dry milk in PBST. Afterwards, the primary antibody (1:500; CFTR (H-182), Santa Cruz) was incubated overnight at 4 °C. For visualization the horseradish-peroxidase bound secondary antibody was added (1:3000), followed by detection with enhance chemiluminescence system (ECL, Pierce).

2.8. Immunofluorescence

Freshly isolated lungs of non-ACTH injected frogs were gently inflated by injecting a 1:2 dilution of Tissue-Tek (Sakura Finetek) and phosphate buffer solution (PBS, pH 7.4). The organs were embedded in Tissue-Tek and shock frozen in isopentane (Roth Chemicals), which was cooled with liquid nitrogen. Cryostat sections (10 μm , Frigocut 2800E, Leica) were mounted on poly-L-lysine-covered glass slides, stored in methanol at 4 °C for 10 min and incubated for 1 h at room temperature. Unspecific binding sites were then blocked by incubation for 1 h with 50% horse serum (diluted with PBS) and the primary antibody (1:100, CFTR (H-182), Santa Cruz) was added overnight at room temperature. Covers were then washed with PBS and incubated for 1 h at room temperature with Cy-3 conjugated donkey anti-rabbit immunoglobulin secondary antibody (1:1000, Chemicon). Finally, sections were treated for 10 min with paraformaldehyde, washed in PBS, embedded in glycerol and evaluated with an epifluorescence microscope (Axioplan 2, Zeiss).

3. Results

3.1. Basic properties of *Xenopus* lung epithelium

The greatest part of the measured current in *Xenopus* lung preparations is sensitive to the diuretic amiloride and represents Na^+ absorption through epithelial Na^+ channels (Fischer et al., 1989; Kim, 1990; Baxendale-Cox, 1999; Fronius et al., 2004). To elucidate the function of luminal CFTR channels in this tissue we used NPPB, NFA, glibenclamide and lonidamine as putative CFTR channel blockers. All blockers were applied to the api-

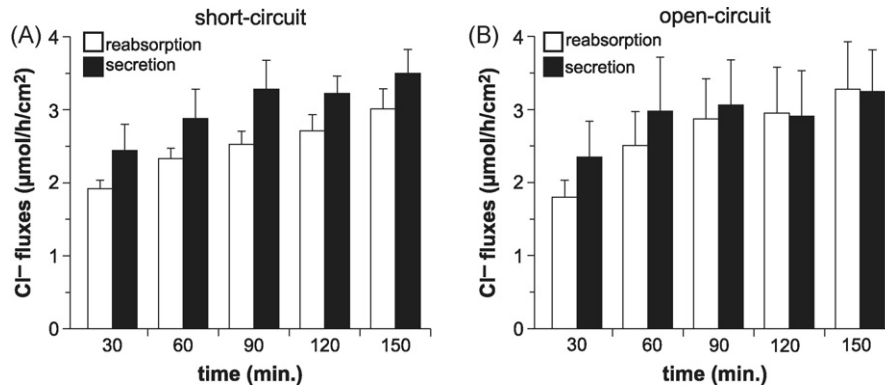


Fig. 1. Unidirectional tracer flux measurements across *Xenopus* lung epithelium. (A) $^{36}\text{Cl}^-$ fluxes were determined under short circuit conditions, indicating a net Cl^- secretion from the basolateral to the apical compartment ($n=4$ for each side, apical to basolateral and basolateral to apical fluxes were determined with preparations derived from one donor). Tissues were allowed to equilibrate for 90 min, then $^{36}\text{Cl}^-$ was added either to the apical or to the basolateral side of the tissues. Samples to determine flux rates were taken in 30 min intervals following $^{36}\text{Cl}^-$ addition. (B) Fluxes determined under open circuit conditions. Under these conditions Cl^- fluxes were reduced compared to the short circuit conditions, although we still observed a net secretion within 90 min after $^{36}\text{Cl}^-$ addition ($n=5$ for each side).

cal side of the tissues and we found that all of them were able to inhibit I_{SC} under basal conditions—independent of the used conditions (short circuit versus open circuit, data not shown). This indicates that this tissue secretes Cl^- via luminal Cl^- conductances. This finding is further supported by unidirectional flux measurements revealing a net $^{36}\text{Cl}^-$ flux from the basolateral to the apical side of the tissues (Fig. 1). Further experiments were performed with the selective CFTR blocker CFTR_{inh}-172 (Ma et al., 2002) and chlorzoxazone, a CFTR activator (Singh et al., 2000).

3.1.1. NPPB and NFA

NPPB and NFA are well-established blockers of different types of Cl^- channels, including CFTR (Schultz et al., 1999). In our experiments apical application of 200 μM NPPB inhibited $18 \pm 3\%$ of the measured baseline current (Fig. 2; $n=9$, $P<0.001$). Similar results were obtained with 300 μM apical NFA ($22 \pm 5\%$, $n=9$, Fig. 2B). Following application of 10 μM amiloride in addition to NPPB, decreased I_{SC} by about $82 \pm 5\%$ (with respect to baseline current without blocker; $n=9$,

$P<0.001$). Although the effect of NPPB was dose-dependent, we found that concentrations above 300 μM induced unspecific inhibition of the I_{SC} accompanied by an obvious decrease of the transepithelial resistance (R_{T}). This unspecific inhibition persists even after NPPB was removed from the apical compartment indicating additional effects as reviewed by Schultz et al. (1999). Therefore, we were not able to determine adequate half-maximal inhibitory concentrations for NPPB (data not shown). Half-maximal inhibition of I_{SC} was determined with 232 μM NFA (see Fig. 3C) (Table 1).

3.1.2. Glibenclamide and lonidamine

Further experiments were performed with glibenclamide and lonidamine, since these two compounds are indicated to be more CFTR selective compared with NPPB and NFA, respectively (Schultz et al., 1999; Gong et al., 2002). Interestingly, apical application of low concentrations ($<250 \mu\text{M}$ lonidamine; $<500 \mu\text{M}$ glibenclamide) slightly increased I_{SC} , whereas lonidamine concentrations $\geq 250 \mu\text{M}$ and glibenclamide concentrations $\geq 500 \mu\text{M}$ inhibited I_{SC} (Fig. 3A and

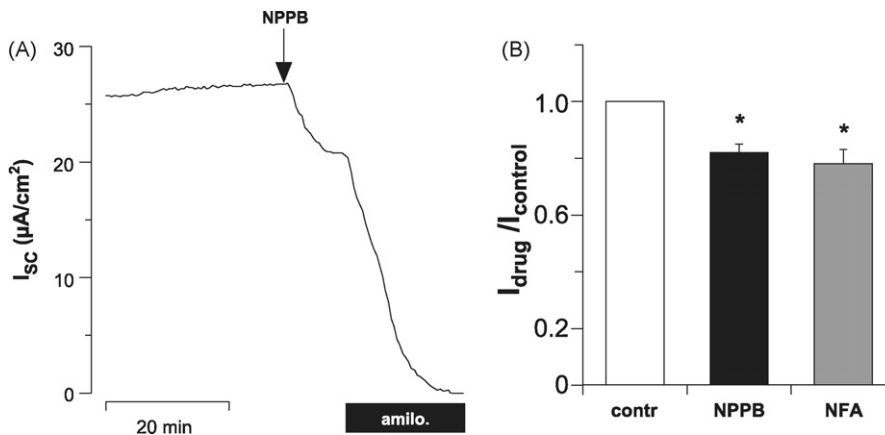


Fig. 2. Effect of NPPB and NFA on short circuit current (I_{SC}) in *Xenopus* lung. (A) Original recording displaying the effect of 200 μM apical NPPB. NPPB induced inhibition saturated within 10–30 min and the remaining current was further blocked by additional amiloride (amilo.; 10 μM .) application. (B) Summarized data of experiments as shown in panel A. NFA was applied in a concentration of 300 μM to the apical side of the tissues (NPPB: $n=9$, $*P<0.001$; NFA: $n=9$, $*P<0.001$). Means (\pm S.E.M.) represent normalized values before (contr., control) and after blocker application.

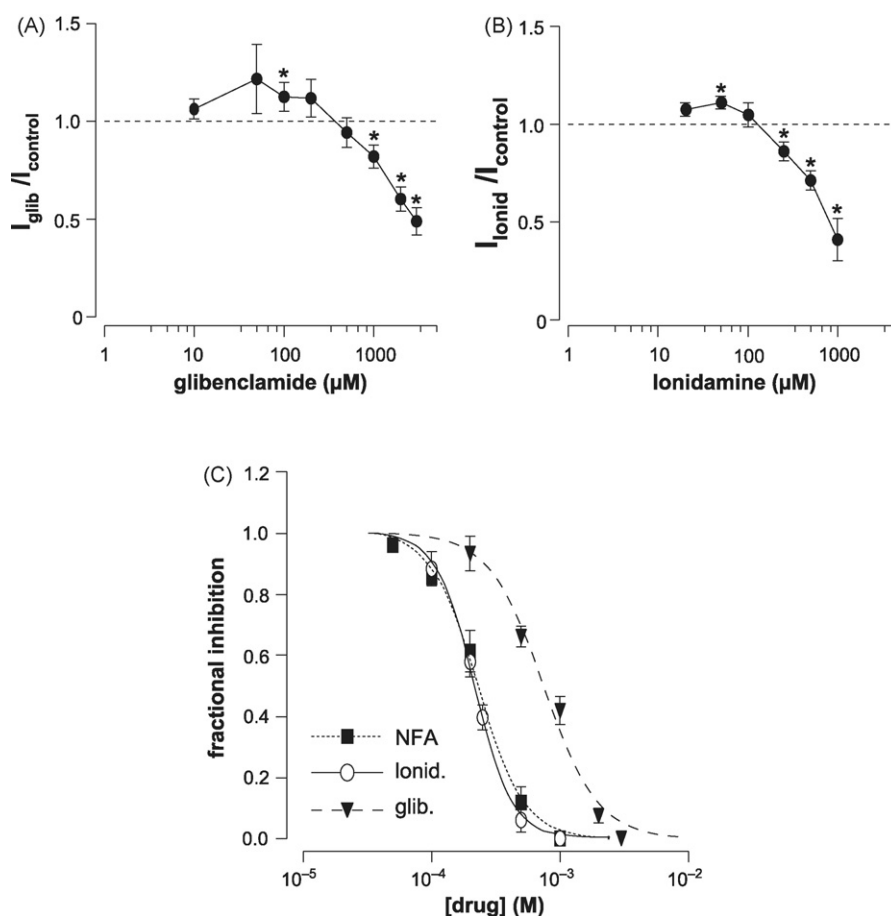


Fig. 3. Dose-dependent effects of designated CFTR inhibitors. (A) Apical glibenclamide concentrations from 10 to 200 μM induced stimulation of I_{SC} , whereas concentrations $\geq 500 \mu M$ inhibited transepithelial currents. Data represent means (\pm S.E.M.) of at least three administrations for each concentration ($n \geq 3$); values were normalized to control conditions represented by the dotted line ($^* P < 0.05$ with respect to control). (B) Lonidamine produced similar results as obtained with glibenclamide. Concentrations from 20 to 100 μM increased I_{SC} , concentrations $\geq 250 \mu M$ obviously decreased the measured current ($n \geq 3$, $^* P < 0.05$ with respect to control). Inhibition of I_{SC} by both drugs is in agreement with inhibition of CFTR mediated Cl^- secretion. (C) Means were plotted and fitted according to the Hill equation to determine IC_{50} values for drug-induced inhibition. IC_{50} values were calculated for NFA with 232 μM , for lonidamine with 218 and for glibenclamide with 748 μM .

B). To determine half-maximal inhibition concentrations, those concentrations were plotted and fitted by Hill equation where an inhibition of the I_{SC} was observed (Fig. 3C). The determined IC_{50} value for lonidamine was 218 μM and for glibenclamide 748 μM (Table 1). At this point one should consider that both compounds were poorly soluble at high concentrations. And although we were able to observe dose-dependent inhibition of I_{SC} , the determined IC_{50} values may not represent adequate pharmacological profiles, since we were not able to distinguish between the added amount of the drugs and the dissolved effective concentration. Nevertheless, the observed net-inhibition with glibenclamide and lonidamine confirm the results obtained with NPPB and NFA concerning Cl^- secretion, further indicating the participation of a CFTR like ion channel.

3.2. Effect of CFTR_{inh}-172 on chlorzoxazone induced currents

Finally, we used the highly selective inhibitor CFTR_{inh}-172 (Ma et al., 2002) in combination with the putative CFTR activator chlorzoxazone (Singh et al., 2000). Because of the poor

solubility of CFTR_{inh}-172 in our experimental solution, the blocker was dissolved in relatively high amounts of DMSO. Final DMSO concentration in the perfusion solution was 1% and in order to avoid side effects of DMSO, 1% DMSO was added to the experimental solution (not shown) before CFTR_{inh}-172 and/or chlorzoxazone was added.

With CFTR_{inh}-172 (5 μM) at the apical side of the tissues we observed a small but significant decrease of the I_{SC} ($9 \pm 2\%$, $n = 7$, $P < 0.01$). Further, the greatest part of the CFTR_{inh}-172 induced inhibition was reversible (Fig. 4B).

Table 1
Summarized values from dose-dependent effects of Cl^- channel inhibitors on *Xenopus* lung epithelia

	IC_{50} (μM)	95% confidence interval of IC_{50} (μM)	Hill coefficient
NFA	232	202–266	–2.43
Lonidamine	218	204–233	–2.96
Glibenclamide	748	573–976	–2.07

Means were plotted and fitted by Prism 4 (GraphPad) according to the Hill equation.

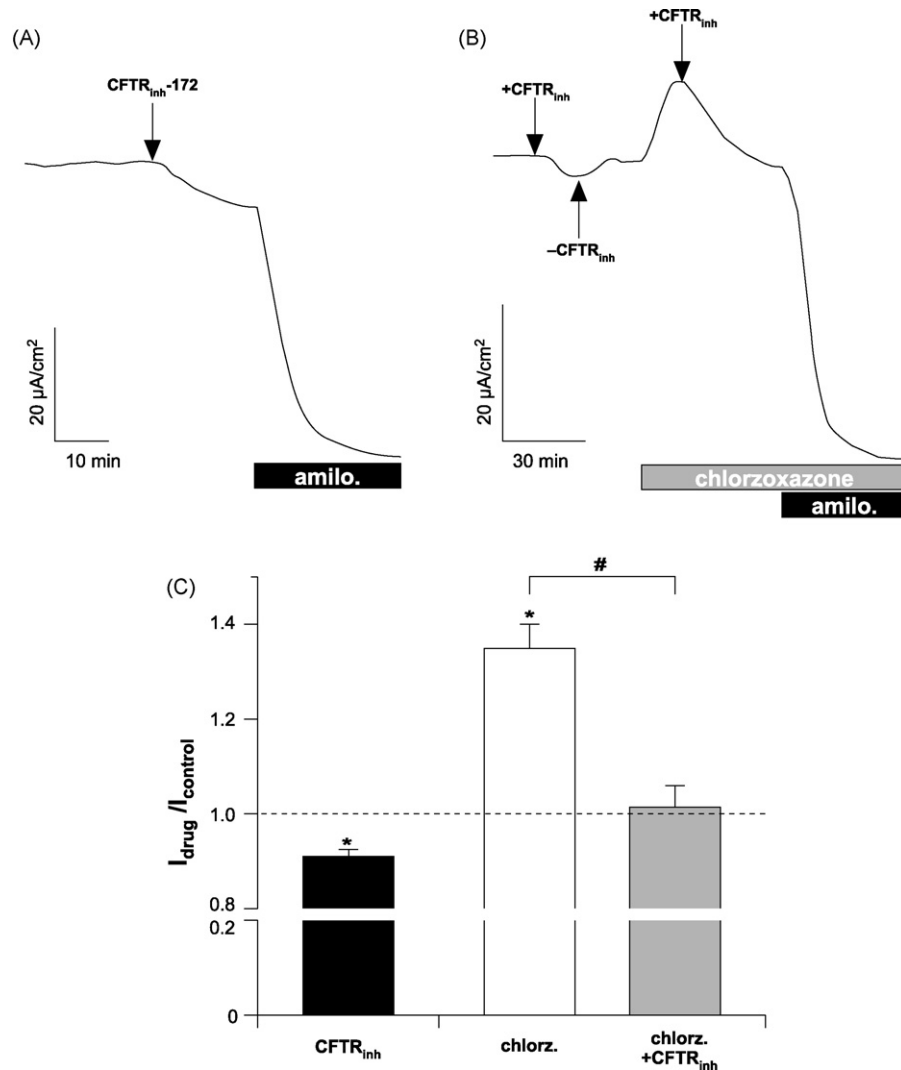


Fig. 4. Effects of CFTR-specific inhibitor and activator on transepithelial I_{SC} . (A) Application of apical CFTR_{inh}-172 (5 μ M) decreased transepithelial I_{SC} under basal (unstimulated) conditions, indicating a Cl^- secretion due to CFTR ion channels. (B) CFTR_{inh}-172 induced effect under basal conditions and following CFTR activation via apical chlorzoxazone (500 μ M) application. Note that the CFTR_{inh}-172 induced inhibition was reversible after wash out of the compound. (C) Summarized data of experiments as shown in panels A and B; values are normalized with respect to control conditions (before drug application) indicated by the dotted line. CFTR_{inh}-172 significantly decreased I_{SC} ($n=7$, $*P<0.01$). Chlorzoxazone (chlorz., 500 μ M) significantly activated a current, which was sensitive to CFTR_{inh}-172 ($n=8$, $*P<0.001$, $\#P<0.001$).

Exposure of the epithelia to 500 μ M chlorzoxazone obviously increased the basal I_{SC} ($35 \pm 5\%$, $n=8$, $P<0.001$, Fig. 4B). Administration of CFTR_{inh}-172 following the chlorzoxazone induced current activation largely inhibited this current ($n=8$, Fig. 4B and C). In some experiments ($n=3$, data not shown) no effect of CFTR_{inh}-172 was detected under basal conditions, but in these cases a CFTR_{inh}-172 sensitive current could be induced with chlorzoxazone.

3.3. Reverse transcription-PCR, Western blots and immunofluorescence

In addition to the electrophysiological studies we used molecular biological techniques to verify the presence of CFTR at RNA and at the protein level. For both approaches freshly iso-

lated lungs were homogenized and samples were used for PCR and antibody detection.

With the used primers, which were designed according to the published sequence of *X. laevis* CFTR (GenBank accession number X65256), we were able to amplify a product with an expected size of 259 bp (Fig. 5A). This finding indicates the presence of a CFTR mRNA within the homogenates of *Xenopus* lung. In addition, Western blot analyses were performed using an antibody against the amino acids 1–182, mapping the N-terminus of human CFTR. With this antibody we detected a characteristic band at the expected size (approximately 160–170 kDa) in samples from lung homogenates but not from oocytes, which were used as negative control (Fig. 5B). Using the same antibody for immunofluorescence detection we found characteristic signals in the apical membranes of the sec-

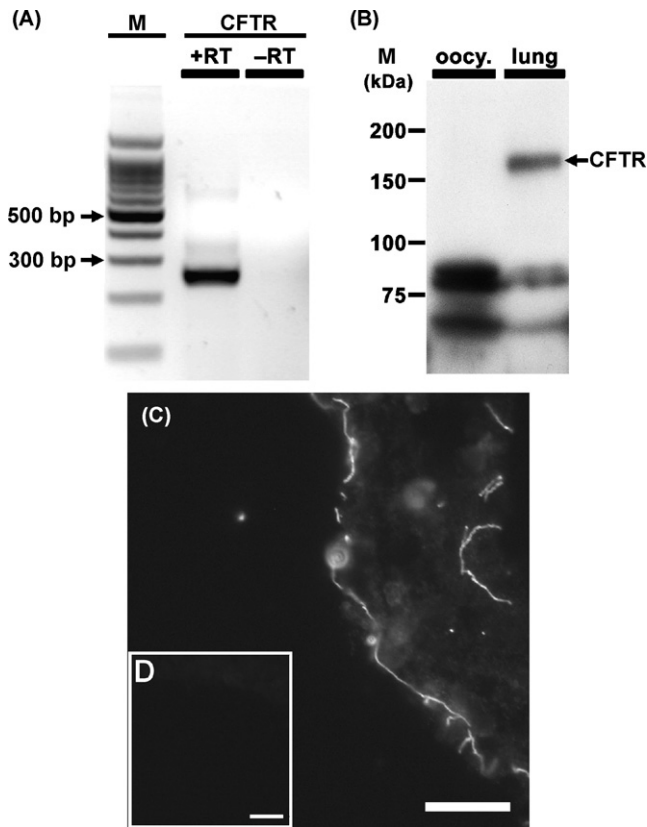


Fig. 5. Molecular identity of a CFTR homolog from *Xenopus* lung. (A) Agarose gel showing the RT-PCR product amplified from *Xenopus* lung homogenates. cDNA derived from total RNA was amplified with primers spanning the region between nucleotides 3995 and 4253 (259 bp fragment). Lane 1: 100 bp marker (M), lane 2: PCR product derived from reverse transcribed RNA (+RT), lane 3: PCR product derived from RNA not reverse transcribed (–RT). (B) Detection of CFTR protein (indicated by arrow) by Western blot analysis from *Xenopus* lung homogenates. With proteins isolated from *Xenopus* lung we were able to detect a characteristic band at the expected size (approximately 160–170 kDa). Samples from *Xenopus* oocytes (oocy.) were used as controls, since there is no evidence for CFTR protein in these well-characterized cells (M: marker). (C) Immunofluorescence staining of *Xenopus laevis* lung slices. With the used antibody we were able to detect characteristic staining of the apical membrane indicating the presence of a CFTR homolog in *Xenopus* pneumocytes. White bar corresponds to 100 μm . (D) Control staining of *Xenopus* where the primary antibody was omitted. In these slices no fluorescence was detected (white bar = 100 μm).

tions. For these studies organs solely from non-ACTH injected animals were used (Fig. 5C).

These data provide clear evidence concerning the transcription, the translation and the localization of a CFTR homolog ion channel in *Xenopus* lung epithelium.

4. Discussion

While the importance of Na^+ absorption as the major driving force to remove fluid from the alveolar airspace is well accepted, the role of Cl^- ion channels in this process has not been established. It remains unclear if the alveolar epithelium secretes or absorbs Cl^- ions (Brochiero et al., 2004; Fang et al., 2006). Gaining further insight on this issue is hampered for two reasons: (a) native mammalian alveolar preparations are recently

not available for electrophysiological measurements under controlled conditions, which of course must be attributed to the complex anatomy of mammalian lungs; (b) the lack of adequate cell culture models, because these models hardly represent the physiological conditions, since a variety of different supplements (including hormones and growth factors) are added to the culture media, thereby influencing the expression of ion channels (Jain et al., 2001; Lazrak et al., 2000a,b). Also time-dependent changes concerning the expression of distinct ion channels were observed (Leroy et al., 2004).

Keeping the usefulness of amphibian tissues (frog skin) and cell culture models (A6 cells) for transepithelial ion transport studies in mind, we tried another approach. We used freshly isolated, native preparations from *Xenopus* lungs for Ussing chamber recordings. Prior studies have already shown that this organ displays several similar features compared with mammalian pulmonary epithelia. Among these are the air–blood barrier (Meban, 1973; Dierichs, 1975; Fischer et al., 1989) and the pneumocytes from *Xenopus* lung, which exhibit morphology of AT I cells combined with functional characteristics of AT II cells (Fischer et al., 1989). The *Xenopus* lung epithelium exhibits active Na^+ reabsorption through amiloride sensitive epithelial Na^+ channels, which were detected (Puoti et al., 1995) and functionally characterized by different groups (Baxendale-Cox, 1999; Kim, 1990; Fischer et al., 1989; Fronius et al., 2003). One basic feature of this tissue is that the effect of blockers on macroscopic currents is relative slow compared with other tissues as mammalian trachea for example. This might be due to the enlarged luminal surface formed by septa (Fischer et al., 1989), reducing the diffusion of applied compounds to distinct parts of the epithelium. Nevertheless, the amiloride sensitive reabsorption observed in this tissue is in accordance with recent suggestions that active Na^+ reabsorption represents the main driving force to remove alveolar fluid in mammalian lungs (Matthay et al., 2002).

In our present study we focused on Cl^- transport and addressed two questions: (a) whether or not *Xenopus* lung may possess a functional CFTR-like ion channel and (b) how this ion channel may contribute to transepithelial ion transport.

Our results using different Cl^- channel blockers clearly indicate, that this tissue exhibits a basal Cl^- secretion. This was further conformed in tracer flux measurements under short circuit as well as open circuit conditions. Although in the open circuit mode the net secretion of $^{36}\text{Cl}^-$ was decreased compared with the secretion under short circuit conditions, we were still able to detect a net secretion within 90 min of incubation (Fig. 1). In the short circuit Ussing chamber measurements, each of the apically applied compounds was able to decrease the transepithelial I_{SC} , which is in accordance with inhibition of luminal Cl^- secretion (Figs. 2–4).

Although each of the used substances blocks CFTR ion channels, it is difficult to conclude that the CFTR ion channel is present only by applying these drugs. NFA and NPPB for example are able to inhibit CFTR ion channels (Schultz et al., 1999; Scott-Ward et al., 2004; Linsdell, 2005) but are also known to block other Cl^- channels (Jentsch et al., 2002). Inhibition of CFTR by NPPB and NFA is suggested to occur via binding to the

inner vestibule of the CFTR channel from the cytoplasmic side (Hwang and Sheppard, 1999; Scott-Ward et al., 2004; Linsdell, 2005). But taking into consideration, that both compounds are able to inhibit different types of Cl^- channels (Jentsch et al., 2002), we cannot exclude inhibition of at least two types of Cl^- channels including CFTR in our experiments.

Glibenclamide and lonidamine in contrast are, so far, indicated to be more selective CFTR inhibitors in comparison to NPPB and/or NFA (Sheppard and Welsh, 1992; Schultz et al., 1999; Gong et al., 2002). Interestingly, we found that both drugs slightly increased I_{SC} when added in relative low concentrations. With increasing concentrations an inhibition of the measured current was observed. The observed increase of I_{SC} by glibenclamide could be reasoned by the inhibition of luminal K^+ channels and/or by activation of ENaC, respectively. Glibenclamide is a very potent inhibitor of K_{ATP} channels (Zunkler et al., 1988) and this type of channel was already described in human alveolar epithelial cells to be involved in luminal K^+ secretion (Sakuma et al., 1998). Thus inhibition of such a secretory K^+ conductance would produce an increase of the transepithelial short circuit current as observed in our study. Another explanation may be a stimulation of apical ENaCs. Different studies were able to demonstrate activation of the *Xenopus* ENaC clone by glibenclamide (Chraïbi and Horisberger, 1999; Schnizler et al., 2003). Unfortunately, at this time we cannot explain the stimulation of the I_{SC} by low concentrations of lonidamine. The interference of lonidamine with distinct K^+ channels has already been demonstrated (Cheranov and Jaggar, 2004), therefore, we cannot rule out such side effects in our experiments. In addition, similar observations concerning activation as well as inhibition of human CFTR were shown with phloxine B (Bachmann et al., 2000; Cai and Sheppard, 2002) and with genistein (Wang et al., 1998) indicating that these compounds may bind to different binding sites of the CFTR molecule and thereby produce opposite effects.

Nevertheless, the observed inhibition of the I_{SC} as detected in our experiments with high concentrations of lonidamine and glibenclamide are in accordance with an inhibition of a CFTR-dependent Cl^- secretion (Fig. 3).

Concerning the half-maximal inhibitory concentrations (IC_{50}) determined from our experiments with NFA, glibenclamide and lonidamine, different aspects should be considered: (a) other ion channels and chloride channels in particular may be involved in the observed inhibition, (b) most of the pharmacological profiles of CFTR inhibitors are achieved from patch-clamp studies in the inside-out configuration, (c) CFTR inhibitors in these patch-clamp recordings were tested under relative high negative voltages and in general these compounds exhibit a greater efficiency at hyperpolarized membrane potentials, (d) almost all inhibitors used in these studies were applied from the cytoplasmic side and thus are easy accessible to the designated binding site (from our recordings it is difficult to determine adequate pharmacological profiles concerning the effective drug concentrations), (e) species-dependent differences in the amino acid sequences may also influence the affinity of the compounds to the ion channel. For example, lonidamine was found to block human CFTR with an IC_{50} value of $58.5 \mu\text{M}$ in inside-out

patches (Gong et al., 2002) but for rat CFTR an IC_{50} value of $631 \mu\text{M}$ was reported on whole cell recordings by the same group (Gong and Wong, 2000).

$\text{CFTR}_{\text{inh-172}}$ is reported to be a highly selective inhibitor of CFTR (Ma et al., 2002; Sheppard, 2004) although the mechanism of inhibition remains to be further elucidated (Taddei et al., 2004). In our study, we found that low concentrations of this compound applied to the apical side of the tissues significantly inhibited the short circuit current under basal conditions (Fig. 4) and that the inhibition was largely reversible as described by other studies (Ma et al., 2002; Wang et al., 2004). In order to further support our assumption concerning a role for CFTR in ion transport participation in this tissue we used chlorzoxazone a compound, which like other benzimidazolones is known to activate CFTR by two different mechanisms: either by a direct interaction with CFTR (Cuthbert, 2001; Caci et al., 2003), or indirect by activation of K^+ channels inducing hyperpolarization and thus increasing the driving force for Cl^- extrusion (Singh et al., 2000). Independent of the underlying mechanism, we found that chlorzoxazone activated a current and this current was sensitive to apical $\text{CFTR}_{\text{inh-172}}$ application. From these results we conclude that the observed increase in I_{SC} is due to an activation of a designated CFTR channel, especially since we were able to block almost the entire chlorzoxazone induced current with $\text{CFTR}_{\text{inh-172}}$ (Fig. 4C). This assumption is further supported by observations that a functional CFTR is required to activate chlorzoxazone induced transepithelial currents, since there was no chlorzoxazone effect detectable in DF508 human airway epithelia (Singh et al., 2000).

In addition to the electrophysiological data, we used molecular and immunofluorescence approaches to detect CFTR transcripts as well as translated CFTR protein. Since the *Xenopus* CFTR homolog was already cloned (Tucker et al., 1992), we used this sequence to create primers for the suggested *Xenopus* CFTR in the lung. These primers produced a band at the predicted size indicating the presence of CFTR ion channel mRNA in the *Xenopus* lung. Further we used an anti-human CFTR antibody directed against the N-terminal region that is conserved between human and *Xenopus* (identity on amino acid level 85%). This antibody also produced a band at the expected size in Western blots, clearly showing the presence of translated CFTR protein in the *Xenopus* lung. This finding is further supported by immunofluorescence staining of the apical membrane using the same antibody. These results are in agreement with a study demonstrating the presence of CFTR mRNA derived from early developmental stages (Tucker et al., 1992) as well as CFTR protein in *Xenopus* skin (Engelhardt et al., 2004). The fact that CFTR homologs were also identified in different non-mammalian vertebrates (e.g. the shark rectal gland, which is a valuable model for Cl^- secreting epithelia; Marshall et al., 1991; Riordan et al., 1994), indicates that this ion channel plays a crucial role in epithelial ion transport and electrolyte homeostasis within the vertebrates.

Taken together, our data indicate that a CFTR homolog is expressed and translated in *Xenopus* lung epithelium. Further we have evidence that this channel is functionally located in the apical membranes of *Xenopus* pneumocytes and contributes to

transepithelial ion transport and thus to the regulation and control of transepithelial water movement. In *Xenopus* lung epithelium, the designated CFTR functions as a secretory ion channel, thus representing the situation known from human fetal alveolar cells (O'Grady and Lee, 2003) as well as from the upper airway epithelia in mammals (Devor et al., 2000). From our present data we suggest that this amphibian tissue may represent a valuable tool for basic pulmonary ion transport studies, exhibiting large similarities compared to mammalian lung epithelia including functional CFTR ion channels and their participation in pulmonary ion transport.

Acknowledgments

We would like to thank M. Buss for excellent technical assistance, Prof. W. Kummer, Dr. K.S. Lips and M. Bodenbenner for their kind support concerning the preparation of the frog lung sections for immunofluorescence staining. Prof. M. Diener and A. Metternich for providing the resources and the know-how for the unidirectional flux measurements. All performed experiments and treatments of the animals were in agreement with the German "Law of Animal Care" (permissions: V54—19c20-15(1) GI 15/7 Nr. 27/01 and II 25.3—19c20-15(1) GI 15/7 Nr. 27/2001 provided by the regional board Giessen). The present study was supported by the Deutsche Forschungsgemeinschaft (DFG) grant FR 2124/1-1.

References

- Bachmann, A., Russ, U., Waldegger, S., Quast, U., 2000. Potent stimulation and inhibition of the CFTR Cl^- current by phloxine B. *Br. J. Pharmacol.* 131, 433–440.
- Baxendale-Cox, L.M., 1999. Terbutaline increases open channel density of epithelial sodium channel (ENaC) in distal lung. *Respir. Physiol.* 116, 1–8.
- Boucher, R.C., 2003. Regulation of airway surface liquid volume by human airway epithelia. *Pflügers Arch.* 445, 495–498.
- Brochiero, E., Dagenais, A., Prive, A., Berthiaume, Y., Grygorczyk, R., 2004. Evidence of a functional CFTR Cl^- channel in adult alveolar epithelial cells. *Am. J. Physiol.* 287, L382–L392.
- Caci, E., Folli, C., Zegarra-Moran, O., Ma, T., Springsteel, M.F., Sammelson, R.E., Nantz, M.H., Kurth, M.J., Verkman, A.S., Galiotta, L.J., 2003. CFTR activation in human bronchial epithelial cells by novel benzoflavone and benzimidazolone compounds. *Am. J. Physiol.* 285, L180–L188.
- Cai, Z., Sheppard, D.N., 2002. Phloxine B interacts with the cystic fibrosis transmembrane conductance regulator at multiple sites to modulate channel activity. *J. Biol. Chem.* 277, 19546–19553.
- Cherhanov, S.Y., Jaggar, J.H., 2004. Mitochondrial modulation of Ca^{2+} sparks and transient KCa currents in smooth muscle cells of rat cerebral arteries. *J. Physiol.* 556, 755–771.
- Chraïbi, A., Horisberger, J.D., 1999. Stimulation of epithelial sodium channel activity by the sulfonylurea glibenclamide. *J. Pharmacol. Exp. Ther.* 290, 341–347.
- Cuthbert, A.W., 2001. Assessment of CFTR chloride channel openers in intact and cystic fibrosis murine epithelia. *Br. J. Pharmacol.* 132, 659–668.
- Devor, D.C., Bridges, R.J., Pilewski, J.M., 2000. Pharmacological modulation of ion transport across wild-type and DF508 CFTR-expressing human bronchial epithelia. *Am. J. Physiol.* 279, C461–C479.
- Dierichs, R., 1975. Electron microscopic studies of the lung of the frog. II. Topography of the inner surface by scanning and transmission electron microscopy. *Cell Tissue Res.* 160, 399–410.
- Dobbs, L.G., 1990. Isolation and culture of alveolar type II cells. *Am. J. Physiol.* 258, L134–L147.
- Donaldson, S.H., Boucher, R.C., 2003. Update on pathogenesis of cystic fibrosis lung disease. *Curr. Opin. Pulm. Med.* 9 (6), 486–491.
- Engelhardt, J.F., Smith, S.S., Allen, E., Yankaskas, J.R., Dawson, D.C., Wilson, J.M., 2004. Coupled secretion of chloride and mucus in skin of *Xenopus laevis*: possible role for CFTR. *Am. J. Physiol.* 267, C491–C500.
- Fang, X., Fukuda, N., Barbry, P., Sartori, C., Verkman, A.S., Matthay, M.A., 2002. Novel role for CFTR in fluid absorption from the distal airspaces of the lung. *J. Gen. Physiol.* 119, 199–207.
- Fang, X., Song, Y., Hirsch, J., Galiotta, L.J., Pedemonte, N., Zemans, R.L., Dolganov, G., Verkman, A.S., Matthay, M.A., 2006. Contribution of CFTR to apical-basolateral fluid transport in cultured human alveolar epithelial type II cells. *Am. J. Physiol.* 290, L242–L249.
- Fischer, H., van Driessche, W., Clauss, W., 1989. Evidence for apical sodium channels in frog lung epithelial cells. *Am. J. Physiol.* 256, C764–C771.
- Fischer, H., Clauss, W., 1990. Regulation of Na^+ channels in frog lung epithelium: a target tissue for aldosterone action. *Pflügers Arch.* 416, 62–67.
- Fronius, M., Clauss, W., Schnizler, M., 2003. Stimulation of transepithelial Na^+ current by extracellular Gd^{3+} in *Xenopus laevis* alveolar epithelium. *J. Membr. Biol.* 195, 43–51.
- Fronius, M., Berk, A., Clauss, W., Schnizler, M., 2004. Ion transport across *Xenopus* alveolar epithelium is regulated by extracellular ATP, UTP and adenosine. *Respir. Physiol. Neurobiol.* 139, 133–144.
- Gong, X.D., Wong, P.Y., 2000. Characterization of Lonidamine and AF2785 blockade of the cyclic AMP-activated chloride current in rat epididymal cells. *J. Membr. Biol.* 178, 225–233.
- Gong, X., Burbridge, S.M., Lewis, A.C., Wong, P.Y., Linsdell, P., 2002. Mechanism of lonidamine inhibition of the CFTR chloride channel. *Br. J. Pharmacol.* 137, 928–936.
- Hwang, T.C., Sheppard, D.N., 1999. Molecular pharmacology of the CFTR Cl^- channel. *Trends Pharmacol. Sci.* 20, 448–453.
- Illek, B., Fischer, H., Clauss, W., 1990. Aldosterone regulation of basolateral potassium channels in alveolar epithelium. *Am. J. Physiol.* 259, L230–L237.
- Jain, L., Chen, X.J., Ramosevac, S., Brown, L.A., Eaton, D.C., 2001. Expression of highly selective sodium channels in alveolar type II cells is determined by culture conditions. *Am. J. Physiol.* 280, L646–L658.
- Jentsch, T.J., Stein, V., Weinreich, F., Zdebik, A.A., 2002. Molecular structure and physiological function of chloride channels. *Physiol. Rev.* 82, 503–568.
- Kim, K.J., 1990. Active Na^+ transport across *Xenopus* lung alveolar epithelium. *Respir. Physiol.* 81, 29–39.
- Knowles, M.R., Boucher, R.C., 2002. Mucus clearance as a primary innate defense mechanism for mammalian airways. *J. Clin. Invest.* 109, 571–577.
- Koefoed-Johnson, V., Ussing, H.H., 1958. The nature of the frog skin potential. *Acta Physiol. Scand.* 42, 298–308.
- Kunzelmann, K., Kathofer, S., Hipper, A., Gruenert, D.C., Greger, R., 1996. Culture-dependent expression of Na^+ conductances in airway epithelial cells. *Pflügers Arch.* 431, 578–586.
- Lazrak, A., Nielsen, V.G., Matalon, S., 2000a. Mechanisms of increased Na^+ transport in AII cells by cAMP: we agree to disagree and do more experiments. *Am. J. Physiol.* 278, L233–L238.
- Lazrak, A., Samanta, A., Venetsanou, K., Barbry, P., Matalon, S., 2000b. Modification of biophysical properties of lung epithelial Na^+ channels by dexamethasone. *Am. J. Physiol.* 279, C762–C770.
- Leroy, C., Dagenais, A., Berthiaume, Y., Brochiero, E., 2004. Molecular identity and function in transepithelial transport of $\text{K}_{(\text{ATP})}$ channels in alveolar epithelial cells. *Am. J. Physiol.* 286, L1027–L1037.
- Linsdell, P., 2005. Location of a common inhibitor binding site in the cytoplasmic vestibule of the cystic fibrosis transmembrane conductance regulator chloride channel pore. *J. Biol. Chem.* 280, 8945–8950.
- Ma, T., Thiagarajah, J.R., Yang, H., Sonawane, N.D., Folli, C., Galiotta, L.J., Verkman, A.S., 2002. Thiazolidinone CFTR inhibitor identified by high-throughput screening blocks cholera toxin-induced intestinal fluid secretion. *J. Clin. Invest.* 110, 1651–1658.
- Marshall, J., Martin, K.A., Picciotto, M., Hockfield, S., Nairn, A.C., Kaczmarek, L.K., 1991. Identification and localization of a dogfish homolog of human cystic fibrosis transmembrane conductance regulator. *J. Biol. Chem.* 266, 22749–22754.

- Matalon, S., O'Brodovich, H., 1999. Sodium channels in alveolar epithelial cells: molecular characterization, biophysical properties, and physiological significance. *Annu. Rev. Physiol.* 61, 627–661.
- Matthay, M.A., Folkesson, H.G., Verkman, A.S., 1996. Salt and water transport across alveolar and distal airway epithelia in the adult lung. *Am. J. Physiol.* 270, L487–L503.
- Matthay, M.A., Clerici, C., Saumon, G., 2002. Invited review: active fluid clearance from the distal air spaces of the lung. *J. Appl. Physiol.* 93, 1533–1541.
- Matthay, M.A., Robriquet, L., Fang, X., 2005. Alveolar epithelium: role in lung fluid balance and acute lung injury. *Proc. Am. Thorac. Soc.* 2, 206–213.
- Meban, C., 1973. The pneumonocytes in the lung of *Xenopus laevis*. *J. Anat.* 114, 235–244.
- O'Grady, S.M., Lee, S.Y., 2003. Chloride and potassium channel function in alveolar epithelial cells. *Am. J. Physiol.* 284, L689–L700.
- Pilewski, J.M., Frizzell, R.A., 1999. Role of CFTR in airway disease. *Physiol. Rev.* 79, S215–S255.
- Puoti, A., May, A., Canessa, C.M., Horisberger, J.D., Schild, L., Rossier, B.C., 1995. The highly selective low-conductance epithelial Na channel of *Xenopus laevis* A6 kidney cells. *Am. J. Physiol.* 269, C188–C197.
- Riordan, J.R., Forbush III, B., Hanrahan, J.W., 1994. The molecular basis of chloride transport in shark rectal gland. *J. Exp. Biol.* 196, 405–418.
- Rubin, B.K., 2002. Physiology of airway mucus clearance. *Respir. Care* 47, 761–768.
- Sakuma, T., Takahashi, K., Ohya, N., Nakada, T., Matthay, M.A., 1998. Effects of ATP-sensitive potassium channel opener on potassium transport and alveolar fluid clearance in the resected human lung. *Pharmacol. Toxicol.* 83, 16–22.
- Schnizler, M., Berk, A., Clauss, W., 2003. Sensitivity of oocyte-expressed epithelial Na⁺ channel to glibenclamide. *Biochim. Biophys. Acta* 1609, 170–176.
- Schultz, B.D., Singh, A.K., Devor, D.C., Bridges, R.J., 1999. Pharmacology of CFTR chloride channel activity. *Physiol. Rev.* 79, S109–S144.
- Scott-Ward, T.S., Li, H., Schmidt, A., Cai, Z., Sheppard, D.N., 2004. Direct block of the cystic fibrosis transmembrane conductance regulator Cl⁻ channel by niflumic acid. *Mol. Membr. Biol.* 21, 27–38.
- Sheppard, D.N., Welsh, M.J., 1992. Effect of ATP-sensitive K⁺ channel regulators on cystic fibrosis transmembrane conductance regulator chloride currents. *J. Gen. Physiol.* 100, 573–591.
- Sheppard, D.N., 2004. CFTR channel pharmacology: novel pore blockers identified by high-throughput screening. *J. Gen. Physiol.* 124, 109–113.
- Singh, A.K., Devor, D.C., Gerlach, A.C., Gondor, M., Pilewski, J.M., Bridges, R.J., 2000. Stimulation of Cl⁻ secretion by chlorzoxazone. *J. Pharmacol. Exp. Ther.* 292, 778–787.
- Taddei, A., Folli, C., Zegarra-Moran, O., Fanen, P., Verkman, A.S., Galiotta, L.J., 2004. Altered channel gating mechanism for CFTR inhibition by a high-affinity thiazolidinone blocker. *FEBS Lett.* 558, 52–56.
- Tucker, S.J., Tannahill, D., Higgins, C.F., 1992. Identification and developmental expression of the *Xenopus laevis* cystic fibrosis transmembrane conductance regulator gene. *Hum. Mol. Genet.* 1, 77–82.
- Wang, F., Zeltwanger, S., Yang, I.C., Nairn, A.C., Hwang, T.C., 1998. Actions of genistein on cystic fibrosis transmembrane conductance regulator channel gating. Evidence for two binding sites with opposite effects. *J. Gen. Physiol.* 111, 477–490.
- Wang, X.F., Reddy, M.M., Quinton, P.M., 2004. Effects of a new cystic fibrosis transmembrane conductance regulator inhibitor on Cl⁻ conductance in human sweat ducts. *Exp. Physiol.* 89, 417–425.
- Whitsett, J.A., 2005. Surfactant proteins in innate host defense of the lung. *Biol. Neonate* 88, 175–180.
- Zunkler, B.J., Lenzen, S., Manner, K., Panten, U., Trube, G., 1988. Concentration-dependent effects of tolbutamide, meglitinide, glipizide, glibenclamide and diazoxide on ATP-regulated K⁺ currents in pancreatic B-cells. *Naunyn Schmiedebergs Arch. Pharmacol.* 337, 225–230.